

Heterogeneous photocatalytic decomposition of saturated carboxylic acids on titanium dioxide powder. Decarboxylative route to alkanes

Bernhard Kraeutler, and Allen J. Bard

J. Am. Chem. Soc., **1978**, 100 (19), 5985-5992 • DOI: 10.1021/ja00487a001 • Publication Date (Web): 01 May 2002

Downloaded from <http://pubs.acs.org> on February 16, 2009

More About This Article

The permalink <http://dx.doi.org/10.1021/ja00487a001> provides access to:

- Links to articles and content related to this article
- Copyright permission to reproduce figures and/or text from this article



ACS Publications
High quality. High impact.

JOURNAL OF THE AMERICAN CHEMICAL SOCIETY

Registered in U.S. Patent Office. © Copyright, 1978, by the American Chemical Society

VOLUME 100, NUMBER 19

SEPTEMBER 13, 1978

Heterogeneous Photocatalytic Decomposition of Saturated Carboxylic Acids on TiO₂ Powder. Decarboxylative Route to Alkanes

Bernhard Kraeutler and Allen J. Bard*

Contribution from the Department of Chemistry, University of Texas at Austin, Austin, Texas 78712. Received March 3, 1978

Abstract: The heterogeneous photocatalytic decomposition of acetic acid/acetate mixtures was studied on n-type TiO₂ powder. The influence of solution composition, reaction temperature, light intensity, and semiconductor properties (crystallographic structure, doping) was investigated. For photodecarboxylation in the absence of molecular oxygen, anatase powders proved to be most efficient with increased reactivity due to doping and/or partial coverage of the powder particles with platinum. The products of the photodecomposition of acetic acid on platinized anatase powder were mainly methane and CO₂, with small amounts of hydrogen and ethane. Other saturated carboxylic acids (propionic, *n*-butyric, *n*-valeric, pivalic, adamantane-1-carboxylic acid) were also photocatalytically decarboxylated to the corresponding alkanes. An interpretation based on the photoelectrochemical properties of n-type TiO₂, with photooxidation and (dark) reduction reactions occurring on the particles on local cell processes, is proposed.

Introduction

Semiconductor materials are of central importance in electrochemical systems which can utilize solar energy for the production of electricity or new chemical species.¹ In photoelectrochemical cells operating in the photovoltaic mode, the light which irradiates the semiconductor-solution interface is converted into electricity ideally with no change in the composition of the solution or the semiconductor material (Figure 1a). The driving force in such a cell is the underpotential developed for an oxidation at the n-type photoanode (or for a reduction at a p-type photocathode). In *photoelectrosynthesis* the light is used to drive an overall cell reaction in a nonspontaneous direction so that the radiant energy is stored as chemical energy (e.g., in fuels) (Figure 1b). Although the original studies in this area were concerned with the photolysis of water (i.e., production of H₂ and O₂),^{2,3} studies of photooxidations of other solution species at n-type semiconductor electrodes have subsequently provided information about the mechanism of such photoassisted processes,⁴⁻⁶ and have been extended to the bulk synthesis of other chemical species.⁷ In *photocatalysis* a reaction is driven in a spontaneous direction by the light; here the radiant energy overcomes the energy of activation of the process (Figure 1c). Cells which operate simultaneously in the photovoltaic and photoelectrosynthetic or photocatalytic modes are also possible.

While photoredox processes in homogeneous solutions are usually inefficient, the electric field (or band bending) at the photoexcited semiconductor-solution interface causes rapid separation of the carriers and thus inhibits recombination of the highly reactive light-generated electron-hole pair. Fur-

thermore, the primary product of electron transfer at the semiconductor-solution interface often does not suffer rapid back-donation of the electron from the electrode, as overpotentials for redox processes involving energy levels in the forbidden band gaps of the semiconductor may be considerable.^{4,7,8} Thus high quantum yields can be obtained in heterogeneous photoredox processes. Moreover, fast, irreversible chemical reactions of the solution species following the electron transfer can compete with the reverse charge transfer at the electrode. With this in mind and to extend the scope of synthetic methods at illuminated semiconductors we investigated a chemical electrosynthetic reaction, the Kolbe decarboxylation of carboxylic acids.⁹ The Kolbe reaction is not an attractive one in the search for an energy-storing system, since the cleavage product, carbon dioxide, renders most simple decarboxylations exoenergetic. Moreover, a high oxidation potential is needed for initiation of the Kolbe reaction on metal electrodes⁹ and many semiconductors (e.g., ZnO, CdS) show limited stability against photodecomposition under strongly oxidizing conditions. Therefore, among the variety of investigated photoinduced oxidation processes at n-type semiconductor materials this decarboxylation reaction has previously received only minor attention.^{4c} We found, however, that the photocatalytic oxidative decarboxylation of acetate to give ethane and carbon dioxide occurs readily and is uncomplicated by electrode decomposition on illuminated rutile electrodes (the photo-Kolbe reaction).¹⁰



A strong correlation has been found between the behavior of photoelectrochemical cells and heterogeneous photocatalytic

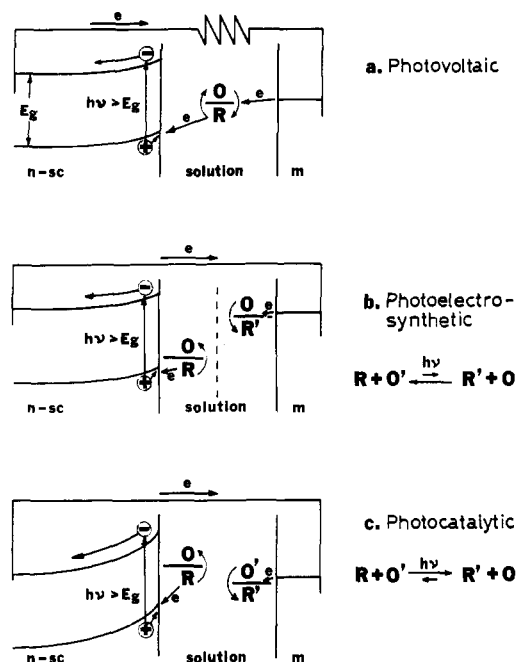


Figure 1. Schematic representations of different types of photoelectrochemical cells and processes: (a) photovoltaic cells, e.g., $n\text{-TiO}_2/\text{NaOH}$, O_2/Pt , or $n\text{-CdS}/\text{S}^{2-}$, $\text{S}_x^{2-}/\text{Pt}$; (b) photoelectrosynthetic, e.g., $\text{SrTiO}_3/\text{H}_2\text{O}/\text{Pt}$ or $n\text{-TiO}_2/\text{OH}^-/\text{H}^+/\text{Pt}$ for production of H_2 and O_2 ; (c) photoelectrocatalytic, e.g. $n\text{-TiO}_2/\text{CH}_3\text{COOH}$, $\text{CH}_3\text{CN}/\text{Pt}$. Long arrows in reactions represent the spontaneous direction ($\Delta G^\circ < 0$). Although cells shown are for n -type semiconductors, equivalent cells for p -type semiconductors have also been formulated.

reactions that occur at semiconductor powders.¹¹⁻¹⁴ Recent applications of particular semiconductors, e.g., TiO_2 and ZnO , to photocatalytic oxidation of cyanide and sulfite¹¹ and other substances^{12,13} have demonstrated the versatility and ease of application of these methods. The clean photodecarboxylation of acetate on rutile electrodes¹⁰ thus suggested a study of the photodecomposition of acetic acid on various TiO_2 powders. The electrochemical measurements on this system^{10,15} have shown that the weak oxidant, H^+ , can serve in the photodecarboxylation reaction, since the photooxidation of acetate on illuminated rutile electrodes occurs at a more negative potential than the onset of the reduction of hydrogen ions in the same acetic acid/acetate mixtures. One of the results, formation of methane from acetic acid, has already been communicated in a preliminary form.¹⁶ Here we report on more extensive studies concerning the photo-Kolbe reaction of acetic acid and of other carboxylic acids. We demonstrate that this reaction appears to be a general method of decarboxylation which is quite simple to use and we propose a mechanism for it.

Experimental Section

Materials. Acetic acid (HAc, glacial, Fisher Scientific Co.), monodeuterioacetic acid (DAC, >98% D, Aldrich Chemical Co.), deuterated water (D_2O , 99.7% d_2 , Merck Sharp & Dohme), propionic acid (Baker grade, Baker Chemical Co.), n -butyric acid (reagent grade, Matheson Coleman and Bell), n -valeric acid (99+, Aldrich Chemical Co.), pivalic acid (99+, Aldrich Chemical Co.), adamantane-1-carboxylic acid (99%, Aldrich Chemical Co.), tetra- n -butylammonium hydroxide (titration grade, 1.0 M in H_2O , Southwestern Analytical Chemical Inc.), acetonitrile (ACN, spectrograde, Matheson Coleman and Bell), n -pentane (spectrograde, Matheson Coleman and Bell) and n -heptane (American Drug & Chemical) were used without further purification. The TiO_2 powders were anatase, undoped (reagent, Matheson Coleman and Bell), confirmed by X-ray to be >99% pure anatase, particle size 125–250 μm and grain size ~ 0.2 μm , geometric surface area $\sim 1\text{--}10$ m^2/g ; doped anatase (produced from the undoped anatase by heating under a hydrogen atmosphere at 650 $^\circ\text{C}$ for 8 h; by X-ray $\sim 10\%$ rutile, $\sim 90\%$ anatase); undoped

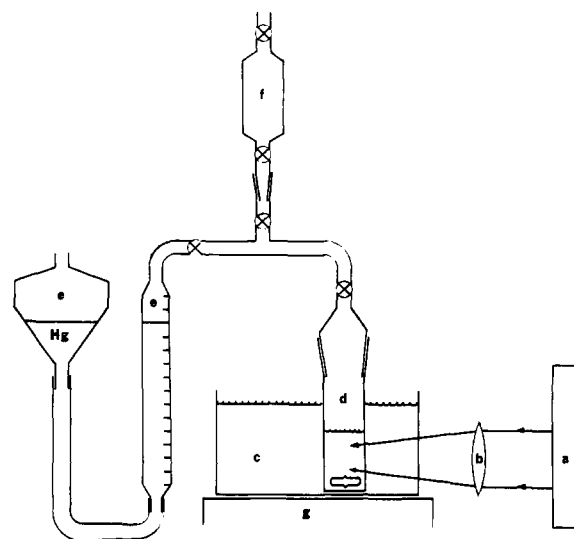


Figure 2. Gas volumetric apparatus for heterogeneous photodecomposition of saturated carboxylic acids (schematic representation): (a) light source; (b) ions; (c) water bath in Pyrex dish; (d) Pyrex reaction cell; (e) gas volumetric system with Hg; (f) gas sample tube; (g) heater-stirrer.

rutile (produced by heating the undoped anatase under air at 1100 $^\circ\text{C}$ for 26 h; by X-ray >99% rutile); doped rutile (produced by heating undoped rutile under H_2 for 12 h at 850 $^\circ\text{C}$). The powders were platinumized by photodecomposition of hexachloroplatinate solutions and contained $\sim 1\text{--}5\%$ platinum by weight.¹⁷

Apparatus. A 2500-W Xe-Hg lamp (Model UF 30 KK,⁹ Christie Electric Corp., Los Angeles, Calif.), operated at 1600 W (hereafter simply called the 2500-W Xe-Hg lamp), was used as the light source for most preparative runs; a 450-W Xe lamp with Model 6242 power supply (Oriell Corp., Stamford, Conn.) served in several analytical runs. The reaction cell and the water bath were both of Pyrex; the bath temperature usually was set to 55 ± 3 $^\circ\text{C}$. Irradiation was performed by illuminating the sample (a stirred suspension of typically 100 mg of powder in 15–20 mL of solution) through the water bath and a flat window on the Pyrex cell. Gas chromatography of reaction gases was done on a Porapak Q column with an Aerograph Hy-Fi Model 600 C instrument. Mass spectral analyses were routinely done on a Model 21-491 Du Pont mass spectrometer. ^1H NMR spectra were taken on a Varian A-60B and ^{13}C NMR spectra were obtained with a Bruker WH-90 instrument.

Product Analysis. Analysis of Gaseous Products. The gases produced during the irradiations under inert atmosphere were collected in a mercury-containing gas volumetric apparatus, shown in Figure 2. The increase of gas volume, as determined at 1 atm and at constant temperature, was taken as the total volume of the gases evolved upon illumination. After termination of each photolysis, a directly attached, evacuated gas sample cell for use in analysis by mass spectrometry was filled with the gas mixture in the volumetric apparatus. At the same time a sample was taken for gas chromatographic analysis (GC). The reaction cell then was uncoupled from the gas volumetric system and purged with nitrogen for ~ 0.5 h. The rate of carbon dioxide evolution was determined gravimetrically in a subsequent run. The reaction gases were swept out of the reaction vessel with a stream of nitrogen and were bubbled through a saturated solution of $\text{Ba}(\text{OH})_2$ in 1 M NaOH. The precipitated BaCO_3 was filtered off, washed well with distilled water, dried at 120 $^\circ\text{C}$, and weighed.

The analytical data for the evolved gas are given below. Mass spectral data¹⁸ employed the most intense signal, that of CO_2 at m/e 44, as the intensity standard (100%). This signal, as well as observed small background signals due to air, water, and solvents, and the helium signal, are not listed below.

Photolysis of Acetic Acid [(10 vol %) in H_2O on platinumized TiO_2]¹⁶: ethane, m/e 30 (2%), 29 (1.5%), 28 ($\sim 7\%$), 27 (2%), 26 (1.5%); methane, m/e 16 (91%), 15 (79%), 14 (5%); hydrogen, m/e 2 (4%). Ratio of methane:ethane from GC, 11:1 (peak height at retention times of 20 and 45 s, respectively).

Photolysis of Monodeuterioacetic Acid [($>98\%$ d_2) on platinumized TiO_2]: ethane, m/e 30 (1.3%), 29 (1.6%), 28 ($\sim 6\%$), 27 (1.5%), 26 (1.1%); methane, m/e 17 (47.3%), 16 (62%), 15 (29%), 14 (4.5%);

Table I. Effect of Concentration and Temperature on Rate of Photocatalytic CO₂ Evolution on Anatase Powder^a

total concn of acetate, M	pH	illumination time, h	BaCO ₃ yield, mg	rate, ^b μmol/h
5	3.4	5	185	190
5 ^c	3.4	3	62 ^c	111 ^c
0.5	3.4	3.75	81	110
0.05	3.4	3.5	64	94
0.02	3.4	2.5	42	86
5	4.7	5	61	62
0.5	4.7	3.2	76	122
0.05	4.7	3.2	77	123
0.02	4.7	1.5	26	87

^a Suspension of 200 mg of undoped anatase in 15 mL of solution; illumination with full output of 2500-W Xe lamp at 55 °C in presence of oxygen. ^b Rate of CO₂ evolution. ^c At 42 °C.

hydrogen, *m/e* 4 (1.8%), 3 (0.5%), 2 (0.9%). Deuterium content: ethane, ~0% deuterium; methane, 80% ± 3% monodeuterated; hydrogen, >60% dideuterated, >17% monodeuterated. Ratio methane:ethane ~15:1 (from GC).

Photolysis of Propionic Acid [(10 vol %) in H₂O on platinumized TiO₂]: ethane, *m/e* 30 (15%), 29 (17%), 28 (~75%), 27 (31%), 26 (24%); hydrogen, *m/e* 2 (17%). Signals due to butane at *m/e* 43 were absent.¹⁹ GC showed a single peak with a retention time of 42 s.

Photolysis of *n*-Butyric Acid [(8 vol %) in H₂O on platinumized TiO₂]: propane, *m/e* 44 (~17%),²⁰ 43 (14%), 42 (7.5%), 41 (14.5%), 40 (2.5%), 39 (9%), 29 (39%), 28 (~31%), 27 (11.5%), 26 (2%); hydrogen, *m/e* 2 (2.5%); no signal at *m/e* 86 due to hexane. GC showed a single peak with retention time of 115 s.

Photolysis of *n*-Valeric Acid [(5 vol %) in H₂O on platinumized TiO₂]: *n*-butane, *m/e* 58 (4%), 43 (50%), 42 (7%), 41 (13%), 39 (4%), 29 (22%), 28 (~18%), 27 (15%); hydrogen, *m/e* 2 (3%); no signal at *m/e* 86 due to *n*-octane. GC showed a single peak with a retention time of 420 s.

Photolysis of Pivalic Acid [(5 vol %) in ACN/H₂O (1:1) on platinumized TiO₂]: isobutane, *m/e* 58 (2%), 57 (3%), 43 (44%), 42 (14%), 29 (4%), 28 (~14%), 27 (12.5%); 2-methylpropene, *m/e* 56 (9%); hydrogen, *m/e* 2 (15%).

Analysis of Nongaseous Products. After the photolysis of pivalic acid an extraction of the reaction mixture with *n*-pentane did not lead to the detection of higher boiling hydrocarbon products.

Photolysis of Adamantane-1-carboxylic Acid (Synthesis of Adamantane). Adamantane-1-carboxylic acid (360 g, 2 mM) was dissolved in 15 mL of ACN and 1.5 mL of *n*-heptane. A 1 M solution (50 μL) of tetra-*n*-butylammonium hydroxide in water and the powdered catalyst (100 mg of platinumized, doped anatase¹⁷) were added. The stirred suspension, contained in a Pyrex cell that was immersed in the water bath at 55 °C, was deaerated with nitrogen and then illuminated with the 2500-W Xe-Hg lamp. After an irradiation time of 27 h, 240 mg of BaCO₃ was collected (representing 1.25 mmol or 62% decarboxylation) and the reaction was stopped. The slightly yellow reaction mixture was extracted with *n*-pentane. The solution was washed with 0.01 N aqueous KOH and the solvent (*n*-pentane) was carefully evaporated under reduced pressure at room temperature. The remaining waxy, white solid (~150 mg) was subjected to sublimation at room temperature and ~0.1 Torr to give adamantane as a colorless, crystalline product in a yield of 95 mg (58%). The product, adamantane, with mp ~263–265 °C (lit.²¹ 270 °C), was identified by its mass spectrum¹⁸ and its ¹H and ¹³C NMR spectra.²²

Results

Photocatalytic Decomposition of Aqueous Acidic Acetate/Sodium Acetate Mixtures on TiO₂ Powders in the Presence of Oxygen. Illumination of suspensions of TiO₂ powders in aqueous acetic acid/sodium acetate mixtures in the presence of 1 atm oxygen leads to the observable evolution of carbon dioxide. In these experiments oxygen was passed through the reaction mixture continuously and was used to carry the volatile reaction products into a saturated solution of Ba(OH)₂

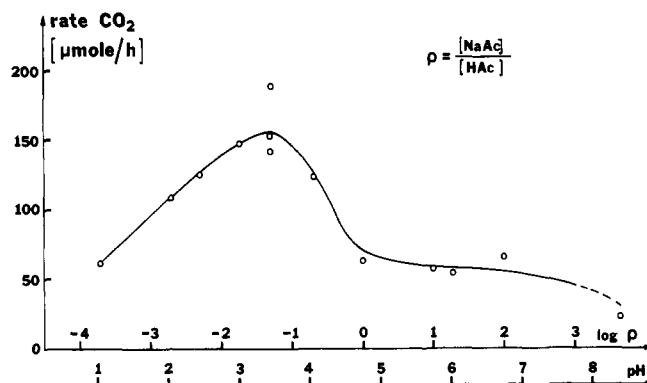


Figure 3. pH dependence of rate of photocatalytic CO₂ formation on 200 mg of undoped anatase in 5 M acetic acid/sodium acetate solution in water at 55 °C and in presence of oxygen.

in 1 M NaOH, causing the CO₂ to be precipitated as BaCO₃. This was weighed and the CO₂ evolution rate determined. The pH dependence of the rate of photocatalytic CO₂ evolution with anatase powder at 55 ± 3 °C using suspensions of 200 mg of catalyst in 15 mL of aqueous solutions containing a constant total concentration (5 M) of acetic acid/sodium acetate is shown in Figure 3. To circumvent as much as possible the use of other buffer mixtures (with some sacrifice of buffering capacity) the ratio acetic acid:sodium acetate was used to establish the pH of the solutions in the pH range 2.4–7. The pH values calculated were based on the concentrations using a pK(HAc) = 4.75.²³ More acidic solutions were prepared by acidification of aqueous acetic acid solutions with a known amount of 1 M H₂SO₄. A 5 M solution of sodium acetate was investigated to give a reactivity value for the most basic solution with an estimated pH of 8–9. Complete removal of CO₂ from the less acidic reaction mixtures was ensured by addition of 4 M HCl after photolysis with continued purging with oxygen and trapping of CO₂ as BaCO₃. The amount of TiO₂ powder used ensured complete adsorption of the light near the flat Pyrex window of the cell, but no studies were done to determine the effect of less TiO₂ catalyst. The stability of the powder was tested in several runs at pH 1.0–4.7, where complete recovery of powder was found even after 10 h irradiation, with production of a total of 840 μmol of CO₂. Typically a run lasted for 5 h, and if repeated with the same powder, reproducibility of the rate of CO₂ evolution was found to be reasonably good (±10%). Several experimental parameters were tested for qualitatively (Tables I and II): a temperature drop from the usual 55 °C to 42 °C brought about a noticeable decrease of CO₂ evolution. On the other hand, at pH 3.4, a decrease of the total acetate concentration from 5 to 0.02 M only decreased the rate by a factor of ~2. At pH 4.7 high acetate concentrations actually seemed to inhibit the CO₂ production. A variety of TiO₂ powders were tested for their activity as photocatalysts for decomposition of acetate in the presence of oxygen. Anatase proved to be somewhat more active than rutile, with little influence of doping, but a significant reactivity increase resulted from partial platinumization of the powders (Table II). Photolysis with the 450-W Xe lamp allowed a rough estimation of the quantum yield of the photodecomposition of acetate on undoped anatase in the presence of oxygen to be made (Table II). The rate of CO₂ evolution, 34 μmol/h, corresponds to a quantum yield of at least 9.5%,²⁴ based on the limiting photocurrent found with a large single crystal rutile electrode, irradiated by the same light source in aqueous solutions, where a quantum yield of ~0.8 can be reached for photooxidation of water.

Specific adsorption of acetate ions from an acetic acid/sodium acetate buffer was found to occur on untreated anatase powder. As expected,²⁶ a deaerated suspension of 1 g of un-

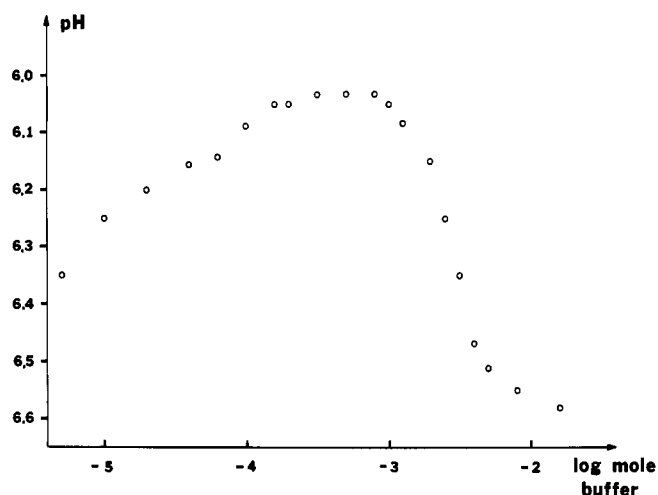


Figure 4. pH of a suspension of 1.00 g of undoped anatase in deaerated water during titration with a 0.1 M acetate buffer at pH 6.62.

Table II. Effect of Catalyst Material on Rate of Photocatalytic CO₂ Evolution in the Presence of Oxygen

catalyst ^a	solution composition ^b	time ^c	yield ^d	rate ^e
none	5 M NaAc/HAc (1:20)	4	2	2.5
TiO ₂ (a,u)	5 M NaAc/HAc (1:20)	5	185	190
TiO ₂ (a,d)	0.5 M NaAc/HAc (1:1)	3	110 ^f	185 ^f
TiO ₂ (r,d)	5 M NaAc/HAc (1:20)	2	27	68
TiO ₂ (a,u,Pt)	0.8 M HAc	2	171	440
TiO ₂ (r,d,Pt)	0.8 M HAc	3.5	70	105
Control Experiments				
TiO ₂ (a,u)	5 M NaAc/HAc (1:20)	12/dark	0	0
TiO ₂ (a,u)	5 M NaAc/HAc (1:1)	4/450 W ^g	27	34
TiO ₂ (a,u)	1 M NaAc/HAc (1:10) +0.2 M H ₂ O ₂	15/dark	25	8.8

^a a = anatase, r = rutile, d = doped, u = undoped, Pt = platinized.¹⁷
^b Total concentration. ^c Irradiation time in hours at 55 °C, light source 2500-W Xe lamp, full output. ^d Yield of BaCO₃ in milligrams. ^e Rate of CO₂ evolution in μmol/h. ^f At 65 °C. ^g Light source 450-W Xe lamp, full output.

doped anatase powder (125–250 μm grain size) in distilled water showed nearly the same pH (6.6) as the distilled water itself (6.7), as determined with a Beckman Expandomatic pH meter using a calibrated glass electrode. Titration of this suspension with a 0.1 M buffer of acetic acid/sodium acetate with pH 6.62 under N₂ initially produced a sharp decrease of the solution pH, reaching a plateau at pH ~6.03 after addition of 2–7.5 mL of the buffer (Figure 4) signaling adsorption of acetate ion. Further addition of buffer finally caused an increase of pH back toward the buffer pH of 6.62, corresponding to a saturation of acetate adsorption of ~1.3 mmol acetate/g anatase.

Analysis of the gases produced by photodecomposition (2500-W Xe–Hg lamp) of acetic acid (10 vol % in H₂O, total 15 mL) on 100 mg of platinized, undoped anatase in the presence of 1 atm oxygen (at 55 °C) revealed CO₂, ethane, and methane as reaction products (ethane:methane ~ 1:12). A comparison of the rate of CO₂ evolution (440 μmol/h) and the rate of increase of the total gas volume (6.6 mL/h) indicated

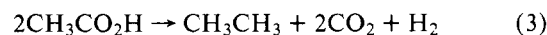
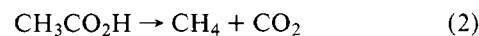
Table III. Effect of Catalyst Material on Rate of Heterogeneous Photocatalytic Decarboxylation of Oxygen-Free Acetic Acid/Sodium Acetate Mixtures^a

catalyst ^b	time ^c	yield of BaCO ₃ ^d	rate ^e	rel rate
r,u	5	2	2	0.15
r,d	5	2	2	0.15
r,d,Pt	3	2.5 ^f	4 ^f	0.31
a,u	6 ^g	15	13	1
a,d	5	58	59	4.5
a,u,Pt	4.75	140	150	11.5
a,d,Pt	1.1 ^h	75 ^h	360 ^h	28
a,d,Pt	2.7	121 ⁱ	230 ⁱ	17.5
a,d,Pt	3.7 ^j	18 ^j	25 ^j	1.9

^a 100 mg of TiO₂ powder in a stirred suspension ~15–20 mL irradiated at 55 ± 3 °C with a 2500-W Xe–Hg lamp, operated at 1600 W, under nitrogen, 1 g of NaAc in 15 mL of HAc. ^b r = rutile, a = anatase, u = undoped, d = doped, Pt = platinized.¹⁷ ^c Time of illumination in hours. ^d Yield in milligrams (error limit ±1 mg). ^e Rate of CO₂ evolution in μmol/h. ^f HAc 10 vol % in H₂O. ^g Light source: 2500-W Xe lamp, full output focused on cell. ^h Pure HAc as solvent. ⁱ At 45 °C. ^j Light source: 450-W Xe lamp, estimated quantum yield 7%.

formation of some nonvolatile products. After correction for the necessary consumption of oxygen (reduction of hydrogen ions to give H₂ was suppressed) the rate of production of volatile hydrocarbons (ethane, methane) represented only ~30% of the rate of decomposition of acetic acid. Methanol and formaldehyde are likely products of the reaction, but their presence was not verified experimentally.

Photocatalytic Decomposition of Oxygen-Free Acetic Acid on TiO₂ Powders. The activity of a variety of n-TiO₂ powders for the photocatalytic decomposition of oxygen-free acetic acid is shown in Table III. In one series of experiments the full output of the 2500-W Xe–Hg lamp, was focused on an area of ~5 cm² on the flat Pyrex window of the reaction vessel. Even with this high light intensity, the amount of suspended powder completely absorbed the light in the front half of the cell. The activity of the powders for the photocatalytic decomposition of acetic acid was again estimated from the yield of CO₂, determined gravimetrically as BaCO₃. As tabulated in Table III, all the rutile powders lead to only little CO₂ evolution. On the other hand, anatase powders were quite reactive photocatalysts in the order undoped < doped < undoped, platinized < doped, platinized. Again a change to a weaker light source, a 450-W Xe lamp, drastically decreased the rate of CO₂ evolution, as did similarly a lowering by 10 °C of the reaction temperature (from 55 to 45 °C). Addition of sodium acetate to the suspensions in acetic acid did not enhance the CO₂ evolution, nor did mixing in of water decrease it, except for high dilution of acetic acid (Table IV). The results of an analysis for all the gaseous reaction products as described in the Experimental Section are given in Table V. The major hydrocarbon product of the heterogeneous photocatalytic decomposition of acetic acid on platinized anatase powder was methane, together with CO₂ (eq 2); only a small amount of hydrogen gas and ethane was found (eq 3).



Ethane, the usual Kolbe product from acetic acid/acetate electrolysis, was formed in only 5–10% yield, with a tendency to an increased fraction of ethane with increasing rate of gas evolution, as clearly established by mass spectrometry and gas chromatography. In the absence of molecular oxygen, side reactions leading to nonvolatile hydrocarbon derivatives (e.g., CH₃OH) were insignificant, as shown by comparison of the

Table IV. Effect of Water on the Rate of Photodecomposition of Oxygen-Free Acetic Acid on Undoped, Platinized¹⁷ Anatase^a

vol % water	illumination time ^b	yield of BaCO ₃ ^b	rate ^b
0	5.5	175	160
5	3.25	110	170
50	3.7	108	153
95	3	71	123

^a Illumination with 2500-W Xe-Hg lamp at 1600 W, 100 mg of catalyst powder in 15 mL of solution, at 55 °C under nitrogen. ^b Illumination time in hours, yield at BaCO₃ in milligrams, rate of CO₂ evolution in μmol/h.

rates of CO₂ evolution and total gas production. In accord with eq 2 or 3 the carbon dioxide amounted to about half of the total gas volume, even for the photodecomposition of acetic acid from reaction mixtures containing only 10 vol % acetic acid in water. To illuminate the mechanistic origin of the fourth hydrogen atom in methane the photodecomposition of monodeuterated acetic acid (DAc, CH₃CO₂D) was studied and the gaseous reaction products were again analyzed by mass spectroscopy for their deuterium content. The absence of detectable deuterium in the ethane formed contrasted sharply with the high degree of monodeuteration of methane and of deuteration of hydrogen gas formed. This was determined by a simulation of the isotopic peak pattern in the mass spectrum. Compared to nondeuterated acetic acid, the photodecomposition of monodeuterated acetic acid resulted in a slower rate of gas evolution (by a factor of ~1.9). Moreover, hydrogen was enriched in the methane formed by a factor of ≥ 10, based on the assumption of >98% monodeuteration in the DAc used.²⁷

Solar Experiment. Solar irradiation also readily photocatalyzed the decomposition of oxygen-free acetic acid on platinized anatase. An air-tight culture flask was filled with 4 L of glacial acetic acid containing 1 g of sodium acetate and its flat bottom (diameter 20 cm, area 314 cm²) was covered with a thin layer of 400 mg of platinized, doped anatase powder (containing ~1% Pt). This reaction mixture was flushed with nitrogen for 16 h at room temperature to remove oxygen. Then the flask was exposed to sunlight.²⁸ A weak stream of nitrogen, constantly purging the reaction mixture, served to keep out O₂ and carried the CO₂ and the other volatile reaction products out of the flask and through a solution of Ba(OH)₂ in 1 M NaOH where a precipitate of BaCO₃ was formed. The amount of BaCO₃ formed was determined regularly and gave a total of 978 mg of BaCO₃ (4.98 mmol). In the absence of oxygen, the rate of decomposition of acetic acid could thus be estimated to be 415 μmol/day or 1.3 μmol/day-cm². A mass spectral and gas chromatographic analysis of the reaction products showed CO₂ and methane; ethane was not found. Moreover, comparison of the weight of the powder before (380 mg) and after the experiment (368 mg) showed good stability of the photocatalyst under the conditions, allowing for the loss of powder on recovery from the large volume of solution.

Photocatalytic Decomposition of Other Saturated Carboxylic Acids on TiO₂ Powders in Oxygen-Free Suspensions. The heterogeneous, photocatalytic decarboxylation of acetic acid was explored in three aprotic solvents (ACN, CH₂Cl₂, C₆H₆) to test for the possibility of expanding this decarboxylation reaction to other saturated carboxylic acids of higher molecular weight. Whereas the rate of CO₂ evolution was lower for the aprotic solvents (Table VI), the decomposition products of acetic acid in ACN were still mainly methane and CO₂, together with ~10% hydrogen and ethane. This was shown in a preparative run, where a mixture of 100 mg of doped, platinized anatase powder, 600 μL of HAc, 80 mg of NaAc, and 20 mL of ACN was irradiated at 55 °C with the

Table V. Product Analysis in the Heterogeneous Photocatalytic Decarboxylation of Oxygen-Free Acetic Acid on TiO₂ Powders^a

solution composition	total gas rate	CO ₂ rate ^b	methane: ethane	D ₂ :HD:H ₂
HAc	4.2 ^c		19:1	0:0:1
HAc 10 vol % in H ₂ O	8.1 ^c	3.5	11:1	0:0:1
HAc	15.5 ^d	8.1	8:1	0:0:1
HAc 10 vol % in D ₂ O	5.6 ^c		15 ^e :1 ^h	<i>i</i>
DAc (>98% D)	8.1 ^d		15 ^f :1 ^h	2:0.6:1 ^j
DAc (95% D)	8.0 ^d	5.1	20 ^g :1 ^h	2:1.1:0.6 ^j

^a 100 mg of TiO₂ powder in 15–20 mL of solution at 55 °C irradiated with 2500-W Xe-Hg lamp operated at 1600 W, under nitrogen. ^b In μmol/h. ^c Catalyst = undoped, platinized anatase. ^d Catalyst = doped, platinized anatase. ^e 73% CH₃D, 27% CH₄ (±1%). ^f 80% CH₃D, 20% CH₄ (±3%). ^g 45% CH₃D, 55% CH₄ (±3%). ^h 100% CH₃CH₃. ⁱ Signal of D₂ was not resolved from the He signal. ^j The H₂ signal lacks significance partially due to decomposition of ionized methane.

Table VI. Effect of Cosolvent on Rate of Heterogeneous Photocatalytic Decarboxylation of Oxygen-Free Acetic Acid on Doped, Platinized Anatase Powder^a

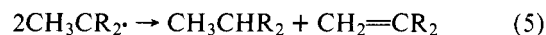
cosolvent	salt	temp, °C	rate of CO ₂ evolution, μmol/h
		55	360
H ₂ O (90 vol %)		55	406
ACN (97 vol %)		36	95
ACN (97 vol %)	NaAc ^b	36	130
CH ₂ Cl ₂ (90 vol %)		30	128
C ₆ H ₆ (90 vol %)		39	50
C ₆ H ₆ (90 vol %)		55	77

^a 100 mg of TiO₂ photocatalyst in 15–20 mL of solution under nitrogen, irradiated with 2500-W Xe-Hg lamp at 1600 W. ^b 80 mg in 20 mL of solution.

2500-W Xe-Hg lamp to give these gases at a total rate of 7.9 mL/h, corresponding to a rate of decarboxylation of ~170 μmol/h. The other saturated carboxylic acids that were investigated are listed in Table VII. In all of these cases the decarboxylation to the corresponding alkane



appeared to proceed cleanly; Kolbe dimers were found only for decarboxylation of acetic acid, as ethane. Side reactions due to disproportionation via H-atom abstraction occurred only for the decarboxylation products of pivalic acid (tetrabutyl radical, R = Me), and the possibility of propionic acid (ethyl radical, R = H)



as shown in the mass spectrum of the reaction gases. In aqueous solutions the rates of decarboxylation were similar for the acids investigated. Adamantane-1-carboxylic acid, dissolved in ACN at a much lower concentration (~0.12 M), was found to decarboxylate at a significantly lower rate than the other acids with a decrease in rate as the photolysis proceeded (initial rate, 65 μmol/h; final rate, after 62% conversion, 28 μmol/h). However, the corresponding alkane, adamantane, was again formed in 58% yield by decarboxylation of this bridgehead carboxylic acid. A noise decoupled ¹³C NMR spectrum showed only two nonequivalent carbon atoms, yielding definite proof of the product, owing to its high symmetry. The usual electrochemical Kolbe reaction for these acids produces predominantly dimer with smaller amounts of the alkene.^{9b} For the

Table VII. Heterogeneous Photocatalytic Decarboxylation of Saturated Carboxylic Acids on Platinized, Doped Anatase Powders^a

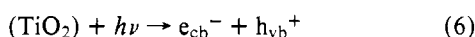
acid	solvent (ratio ^b)	yield of gas ^c	major products	minor products
acetic acid		15.5	CH ₄ , CO ₂	CH ₃ CH ₃ , H ₂
acetic acid	H ₂ O (1:10)	8.1 ^d	CH ₄ , CO ₂	CH ₃ CH ₃ , H ₂
propionic acid	H ₂ O (1:10)	19	CH ₃ CH ₃ , CO ₂	CH ₂ =CH ₂ , H ₂
<i>n</i> -butyric acid	H ₂ O (1:12)	9.4	propane, CO ₂	H ₂
<i>n</i> -valeric acid	H ₂ O (1:20)	16	<i>n</i> -butane, CO ₂	H ₂
pivalic acid	ACN/H ₂ O(1:10:10)	6	isobutane, CO ₂	isobutylene, H ₂
adamantane-1-carboxylic acid	<i>e</i>	65 μmol/h ^f	adamantane, CO ₂	

^a 100 mg of TiO₂ powder in a 20-mL solution, at 56 ± 3 °C, under N₂, illumination with 2500-W Xe-Hg lamp at a power level of 1600 W. ^b Volume ratio. ^c In mL/h. ^d Catalyst was undoped, platinized anatase. ^e 360 mg of adamantane-1-carboxylic acid (2 mmol) in 15 mL of ACN and 1.5 mL of *n*-heptane. ^f Yield of CO₂.

adamantane-1-carboxylic acid the Kolbe reaction, carried out in an alcoholic medium at a metal electrode, produces 1-alkoxyadamantane.

Discussion

In the presence of oxygen, several *n*-type semiconductor powders have been shown to behave as photocatalysts and promote the oxidation of substrates.¹¹⁻¹⁴ A tentative model for the behavior of the powders can be proposed based on the electrochemical responses (e.g., current-potential curves) for the same solution species on *n*-type semiconductor electrodes (single crystal, polycrystalline, sintered, or chemically vapor deposited²⁹) of similar material.^{11,14,16} Light of energy greater than the semiconductor band gap (for TiO₂, 3.0-3.3 eV, depending on the form^{24,25}) excites an electron from the valence band into the conduction band, creating an electron-hole pair.



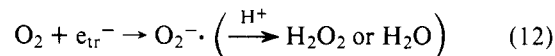
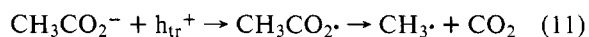
When the redox potential of the solution is positive of the flat-band potential, V_{fb} (e.g., for a TiO₂ electrode in contact with a solution containing an oxidizing species, such as oxygen), the bands at the interface will be bent and the electric field in the space charge region will promote separation of the electron and hole. Some band bending probably also occurs at the powder-solution interface, even for a lightly doped powder. Trapping of the separated charges in shallow traps at the surface is also likely:



The presence of such trapped carriers is suggested by ESR studies of TiO₂ powders and the effect of irradiation on the signals observed,³¹ where species such as O₂^{•+} (which could represent h_{tr}⁺) and Ti³⁺ and O₂^{•-} (which could represent e_{tr}⁻) are proposed. Adsorbed acetate ion could also provide a site for trapping the hole. These trapped carriers can recombine or h_{tr}⁺ can be scavenged by oxidizable species, R (e.g., CH₃CO₂⁻), and e_{tr}⁻ by reducible species, O' (e.g., O₂), in the solution.



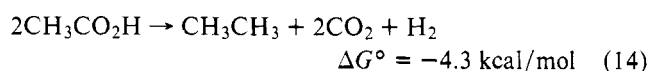
These processes tend to restore the semiconductor powder to its original state. Molecular oxygen is a very convenient oxidizing agent for most photocatalytic oxidations since it is readily available by exposure of the powder to air. The initial steps in the photocatalytic oxidation of acetic acid/acetate mixtures in the presence of oxygen can thus be formulated as



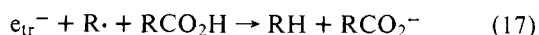
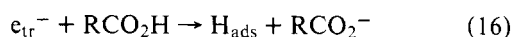
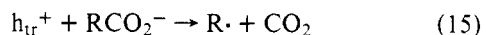
The photocatalytic decarboxylation of acetic acid/acetate on TiO₂ powders in the presence of oxygen is very efficient even at low substrate concentration. The catalytic activity of the anatase powder is highest around pH ~3 for concentrated acetate mixtures. In contrast to methanol and 2-propanol photooxidation on rutile powder,¹³ where the rate increases with decreasing pH and significant reaction occurs only at pHs below 7-8, a considerable amount of acetate oxidation occurs over the entire pH range investigated (pH 1 to ~9). On the other hand, the course of a Kolbe reaction, with hydrocarbon products, is severely disturbed by the presence of molecular oxygen. Formation of ethane and/or methane from acetic acid is largely suppressed by O₂, presumably via reaction of O₂ with the intermediate radicals (probably to give methanol and possibly formaldehyde, by analogy with the formation of alcohols and aldehydes in the electrooxidation of carboxylic acids in the presence of O₂³⁰). To minimize such side reactions, O₂ was replaced by other oxidizing agents. In the absence of O₂ (and without the addition of other oxidizing agents), the proton is the strongest electron acceptor in a heterogeneous photocatalytic cycle with acetic acid/acetate mixtures. The equilibrium potential of the reaction 2H⁺ (solv) + 2e → H₂ (1 atm) is slightly negative of V_{fb} of rutile,³² independent of the pH of the aqueous solution. Consequently, hydrogen evolution in an unbiased photoelectrochemical cell with a rutile photoanode has not been observed.³³ Current-potential curves on rutile electrodes in acetic acid/acetate mixtures show that V_{fb} is negative of the potential for the onset of hydrogen ion reduction on rutile, and even more negative than potentials for the reduction on Pt.^{15,16} The magnitudes of the expected photocurrents for a short-circuited Pt/*n*-TiO₂ (rutile) electrode pair in acetic acid/acetate mixtures were estimated to be rather small¹⁶ and correspondingly rutile powders proved to be rather inefficient in the photocatalytic decomposition of deoxygenated acetic acid. The anatase form of TiO₂ has a somewhat larger band-gap energy than rutile ($E_g = 3.23$ vs. 3.02 eV, respectively²⁴). The Pt/*n*-TiO₂ (anatase) powder showed a much higher reactivity, presumably because of a more negative V_{fb} , even with the smaller efficiency for light-induced electron-hole generation (since a smaller fraction of the incident light is absorbed by the powder). Doping significantly increased the reactivity of the anatase powders for photodecomposition of deoxygenated acetic acid mixtures. As doping affects the bulk properties (conductivity, position of Fermi level) and surface properties (thickness of space charge region, existence and concentration of surface states) of semiconductors, we are not able at the moment to interpret clearly this effect. In particular, surface states can act as mediators in electron transfer reactions⁶ but can also act as recombination centers of the photo-generated electron-hole pairs, thus decreasing the reactivity of the powder as photocatalyst.¹¹ Another source of ineffi-

ciency is the slow rate of reduction of protons on the TiO₂ powders compared to Pt, i.e., on rutile the reduction of protons requires a considerable overpotential. A similar overpotential for hydrogen ion reduction was also found with SrTiO₃³⁴ for potentials positive of V_{fb} . In an n-type semiconductor photoelectrochemical cell the reduction of oxidized species takes place at the metallic counter electrode, while the photocatalytic activity of a semiconductor powder relies on oxidation and reduction processes occurring on the same particle. Therefore, a particle exhibiting both the ability to photooxidize an oxidizable substrate and also to reduce at a high rate an oxidant (such as H⁺) in the dark is required. Such a material was obtained here by combining the n-type semiconductor and Pt on the same particle. Accordingly partial platinization¹⁷ of the powders yielded the most reactive photocatalysts; each grain of platinized TiO₂ represented a short-circuited semiconductor and platinum electrode pair (Figure 5). In the experiments reported here, little formation of hydrogen gas is observed, so actually the platinum sites do not promote efficient hydrogen evolution³⁴ but serve rather as sites for other reduction processes. A strong component of the driving force for the photocatalyzed reaction is the rapidity and irreversibility of the radical decarboxylation.

A problem with photoinduced redox processes at particulate semiconductors is the possibility of "short-circuiting" of the desired overall reaction by the oxidation product (O, in Figures 1b and 1c) being reduced at the cathodic site, because it may be more readily reduced than species O'. This could be a problem, for example in the attempted photodecomposition of water to H₂ and O₂, when the O₂ produced at the photoanodic site (e.g., an n-type semiconductor) is preferentially reduced at a neighboring cathodic site (e.g., a metal or p-type semiconductor). Similarly the catalysis of the back reaction, which is thermodynamically favored in photoelectrosynthesis (Figure 1b), could occur at the particle surface. Rapid decarboxylation of the alkoxy species prevents back reduction in this case. The overall reactions in the simple photo-Kolbe decarboxylations are exothermic:²³



As the major general process is a sequence of oxidation and reduction steps (RCO₂⁻ to R· and CO₂; R· to RH), the required net formation of hydrogen is small. Without detailed knowledge concerning the site and the sequence of the chemical steps in the reduction reaction leading to the monomeric alkanes, the following mechanistic scheme seems appropriate: reactions 6–8 then



Support for this mechanistic scheme is found in the following experimental results:

(a) Electrochemical measurements show that photooxidation of acetate occurs on rutile electrodes at potentials where reduction of hydrogen ions from the same mixture takes place on Pt.^{15,16}

(b) Activity changes of the anatase powders due to partial platinization can be rationalized on the basis of known semiconductor photoelectrochemical cell behavior.

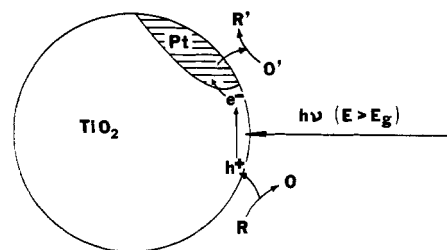


Figure 5. Schematic representation of a photocatalytic reaction on a platinized semiconductor powder particle.

(c) Direct photoexcitation of saturated carboxylic acids occurs only at short wavelengths (i.e., a weak $n \rightarrow \pi^*$ absorption with $\lambda_{\text{max}} \sim 210 \text{ nm}$),³⁶ whereas gas evolution from the TiO₂ powders begins at wavelengths characteristic of the band gap of the semiconductor.²⁴

(d) The photocatalytic decarboxylation is not specific for TiO₂; illumination of a suspension of WO₃ in aqueous acetic acid/acetate mixtures in presence of O₂ also leads to CO₂ evolution.³⁷ For anatase powders no loss of catalyst material during photolysis was noted.

(e) The postulated hydrocarbon radical intermediates have been observed by ESR.³⁸

(f) The decomposition of monodeuterated acetic acid (CH₃CO₂D) produces CH₃D in high yield, thus excluding a direct hydrogen atom abstraction (CH₃· + CH₃CO₂D → CH₄ + ·CH₂CO₂D) as the important reaction in contrast to similar isotopic labeling experiments in the electrochemical Kolbe reaction³⁹ where evidence for abstraction from the methyl group of the acetic acid was found for the methane produced in a side reaction.

(g) The reaction is not specific for acetic acid; all of the investigated saturated carboxylic acids gave the same type of decarboxylation products (eq 4).

As concerns the mechanistic scheme (eq 6–8, 15–20), the postulated possibility of reducing the intermediate hydrocarbon radicals (eq 17) may appear surprising. Recently quite negative reversible potentials were found for the reduction of hydrocarbon radicals in ACN, with $E_{1/2} \sim -2.56 \text{ V vs. SCE}$ for the free *tert*-butyl radical.⁴⁶ The potential for the reduction of methyl radical was estimated to be only slightly less negative in the same aprotic solvent.⁴⁰ Since V_{fb} of TiO₂ (rutile) is about -1.0 V vs. SCE in ACN, and V_{fb} for anatase is probably only a few tenths of a volt more negative, the driving force appears insufficient for reduction of R· at the TiO₂ powders in this solvent. Fast follow-up reactions (protonation of the carbanion) and other stabilizing factors, such as solvation with a protic solvent and adsorption of the carbanion intermediates on the particle surface, can be cited as important factors which could enhance the reduction step with respect to rate and thermodynamic accessibility. An adsorbed radical would resemble a surface state and fast electron transfer to fill this state could be possible, followed by irreversible hydrolysis, i.e.,



Direct reaction of the alkyl radicals with adsorbed hydrogen atoms (eq 20) would be an alternative.

The photodecomposition of carboxylic acids on n-TiO₂ powders (and other large band-gap semiconductors) involve several unique features.

(a) The large catalyst surface area results, at reasonable light intensities, in low surface concentration of the radicals. This inhibits reactions second order in the radical (dimerization, disproportionation). Moreover, the radicals are produced near reducing sites on the powder, as contrasted to methyl

radical production at a separated TiO₂ electrode in a photoelectrochemical cell¹⁰ where ethane is the major product of the photo-Kolbe reaction.

(b) Overall 2e⁻ photooxidations are unlikely. Very strongly reducing intermediates, which are oxidizable at potentials more negative than V_{fb} , could be oxidized by electron transfer to unfilled levels in the conduction band (i.e., in a current doubling process).

(c) The photogenerated holes have energies near the valence band edge and hence are strong oxidizing agents (e.g., for rutile in these solutions at ~+2 V vs. SCE). The electrons at the same time have energies near the conduction band (i.e., near V_{fb}) and show significant reducing power at locations on the particle near the oxidation state. Photoexcited n-type semiconductor powders can thus induce fast oxidation-reduction sequences in reactions that show no overall change of oxidation state.⁴¹ A close parallel between heterogeneous redox reactions on semiconductors and sensitized homogeneous photochemical reactions seems to exist (many photochemical energy transfer reactions are thought to occur via partial charge transfer⁴² and on the other hand electrogenerated cation radicals of carbonyl compounds have been demonstrated to sometimes mimic photochemical reaction steps⁴³). Actually such a relationship is well documented in the photoinduced decarboxylation of carboxylic acids. Similar to the results here presented, photo(sensitized) decomposition of carboxylic acids in the UV region leads to high yield of alkane (and CO₂).⁴⁴

(d) The use of semiconductor powders rather than electrodes gives an added degree of flexibility of the choice of materials, since high conductivity is not required and fabrication problems are avoided. For example, anatase, which is too highly resistive to be used as an electrode, has proven very useful as a catalyst material in this and previous studies.⁶ The photoelectrochemical cell arrangement has the advantage, however, in the separation of the oxidized and reduced materials, which can be particularly important in photoelectrosynthetic applications.

There are a number of possible applications of this photo-decarboxylation reaction. The synthetic scope seems wide. Not only the decarboxylation of acetic acid, but that of all of the other carboxylic acids investigated, gives the same predominant reaction pattern with the corresponding alkane as the main product. This is even true for tertiary and bridgehead carboxylic acids, which are difficult to decarboxylate thermally. Applications to the treatment of waste streams of acetate or other carboxylates, as has been suggested for cyanide and sulfite,⁶ are possible. Synthetic methods involving trapping of the photogenerated alkyl radicals with suitable reagents are also of interest.

Acknowledgment. The support of this research by the Schweizerische National Fonds zur Foerderung der Wissenschaftlicher Forschung (to B.K.) is gratefully acknowledged.

References and Notes

- (a) H. Gerischer, *J. Electroanal. Chem.*, **58**, 263 (1975); (b) M. D. Archer, *J. Appl. Electrochem.*, **5**, 17 (1975); (c) A. Heller, Ed., "Semiconductor Liquid-Junction Solar Cells", Proceedings Vol. 77-3, The Electrochemical Society, Princeton, N.J., 1977, and references cited therein.
- (a) A. Fujishima and K. Honda, *Bull. Chem. Soc. Jpn.*, **44**, 1148 (1971); (b) A. Fujishima and K. Honda, *Nature (London)*, **238**, 37 (1972).
- (a) H. Yoneyama, H. Sakamoto, and H. Tamura, *Electrochim. Acta*, **20**, 341 (1975).
- (a) H. Gerischer in "Physical Chemistry, an Advanced Treatise", Vol. IXA, H. Eyring, D. Henderson, and W. Jost, Ed., Academic Press, New York, N.Y., 1970; (b) H. Gerischer, *Ber. Bunsenges. Phys. Chem.*, **77**, 771 (1973); (c) H. Gerischer and H. Roessler, *Chem.-Ing.-Tech.*, **42**, 176 (1970).
- (a) E. C. Dutoit, F. Cardon, and W. P. Gomes, *Ber. Bunsenges. Phys. Chem.*, **1285** (1976); (b) A. Fujishima, K. Kohayakawa, and K. Honda, *J. Electrochem. Soc.*, **122**, 1487 (1975); (c) K. Nakatani and M. Tsubomura, *Bull. Chem. Soc. Jpn.*, **50**, 783 (1977).
- (a) S. N. Frank and A. J. Bard, *J. Am. Chem. Soc.*, **97**, 7427 (1975); P. A. Kohl and A. J. Bard, *ibid.*, **99**, 7531 (1977).
- (a) S. N. Frank and A. J. Bard, *J. Am. Chem. Soc.*, **99**, 4667 (1977).
- (a) M. Gleria and R. Memming, *J. Electroanal. Chem.*, **65**, 163 (1975).
- (a) H. Kolbe, *Justus Liebigs Ann. Chem.*, **69**, 257 (1849); (b) I. H. P. Utley in "Technique of Electroorganic Synthesis", Vol. 1, N. L. Weissberger, Ed., Wiley-Interscience, New York, N.Y., 1974, p 793; (c) L. Ebersson in "Organic Electrochemistry", M. M. Baizer, Ed., Marcel Dekker, New York, N.Y., 1973.
- B. Kraeutler and A. J. Bard, *J. Am. Chem. Soc.*, **99**, 7729 (1977).
- (a) S. N. Frank and A. J. Bard, *J. Am. Chem. Soc.*, **99**, 303 (1977); (b) S. N. Frank and A. J. Bard, *J. Phys. Chem.*, **81**, 1484 (1977).
- T. Wantanabe, T. Takizawa, and K. Honda, *J. Phys. Chem.*, **81**, 1845 (1977).
- (a) M. Miyake, H. Yoneyama, and H. Tamura, *Denki Kagaku*, **45**, 411 (1977); (b) M. Miyake, H. Yoneyama, and H. Tamura, *Bull. Chem. Soc. Jpn.*, **50**, 1492 (1977).
- T. Freund and W. P. Gomes, *Catal. Rev.*, **3**, 1 (1969).
- B. Kraeutler and A. J. Bard, manuscript in preparation.
- B. Kraeutler and A. J. Bard, *J. Am. Chem. Soc.*, **100**, 2239 (1978).
- B. Kraeutler and A. J. Bard; details of the preparation and characterization of this material will be given elsewhere.
- All mass spectral references values are from E. Stenhagen, S. Abrahamson, and F. W. McLafferty, Ed., "Registry of Mass Spectral Data", Vol. 1, Wiley, New York, N.Y., 1974.
- The signal pattern at m/e 26-30 indicates the presence of a smaller quantity of ethylene.
- Intensity of the second less intense spike at m/e 44.
- P. v. R. Schleyer, *J. Am. Chem. Soc.*, **79**, 3292 (1957).
- R. C. Fort, Jr., in "Studies in Organic Chemistry", P. G. Gassmann, Ed., Vol. 5, Marcel Dekker, New York, N.Y., 1976.
- "CRC Handbook of Chemistry and Physics", 53rd ed, Chemical Rubber Publishing Co., Cleveland, Ohio, 1972.
- An action spectrum, as determined by photoacoustic spectroscopy, for the decomposition of acetic acid on various TiO₂ powders showed the photocatalytic gas evolution to occur at wavelengths shorter than band gap energy. The band gap of anatase powder was found to be ~0.2 eV larger than that of rutile, in agreement with previously reported values (ref 25). (R. C. Gray, B. Kraeutler, and A. J. Bard, *Anal. Chem.*, submitted.)
- V. N. Pak and N. G. Ventov, *Russ. J. Phys. Chem. (Engl. Transl.)*, **49**, 1489 (1975), report E_g (anatase) = 3.23 eV and E_g (rutile) = 3.02 eV.
- (a) P. W. Schindler and S. H. Gamsjaeger, *Kolloid Z. Z. Polym.*, **250**, 759 (1972); (b) M. Herrmann and H. P. Boehm, *Z. Anorg. Allg. Chem.*, **368**, 73 (1969).
- Controls by mass spectroscopy to give more accurate values for the deuterium content of the starting material gave lower deuterium values due to rapid exchange of acidic hydrogens in the mass spectrometer.
- This experiment was carried out from Oct 8 to Oct 20, 1977 (12 days) with partially cloudy weather and temperature highs of 25 °C.
- K. L. Hardee and A. J. Bard, *J. Electrochem. Soc.*, **124**, 215 (1977).
- J. E. Barry, M. Finkelstein, E. A. Mayeda, and S. D. Ross, *J. Am. Chem. Soc.*, **98**, 8098 (1976).
- See, e.g., S. Fukuzawa, K. M. Sancier, and T. Kwan, *J. Catal.*, **11**, 364 (1968); H. Courbon, M. Formati, and P. Pichat, *J. Phys. Chem.*, **81**, 550 (1977).
- M. S. Wrighton, D. S. Ginley, P. T. Wolczanski, A. B. Ellis, D. L. Morse, and A. Linz, *Proc. Natl. Acad. Sci. USA*, **72**, 1518 (1975).
- M. S. Wrighton, A. B. Ellis, P. T. Wolczanski, D. L. Morse, H. B. Abrahamson, and D. S. Ginley, *J. Am. Chem. Soc.*, **98**, 2774 (1976).
- M. S. Wrighton, P. T. Wolczanski, and A. B. Ellis, *J. Solid State Chem.*, **22**, 17 (1977).
- Compare similar results in ref 34.
- M. Simonetta and S. Carra in "The Chemistry of Carboxylic Acids and Esters", S. Patai, Ed., Interscience, New York, N.Y., 1969.
- B. Kraeutler and A. J. Bard, unpublished results.
- B. Kraeutler, C. D. Jaeger, and A. J. Bard, *J. Am. Chem. Soc.*, submitted.
- K. Clusius and W. Schanzer, *Z. Phys. Chem. (Leipzig)*, **192A**, 273 (1943).
- R. Breslow and J. L. Grant, *J. Am. Chem. Soc.*, **99**, 7746 (1977).
- p-Type semiconductor powders should be able to induce similar reactions with the reversed sequence photoreduction-oxidation.
- See, e.g., M. Gordon and W. R. Ware, Ed., "The Exciplex", Academic Press, New York, N.Y., 1975, and references cited therein.
- See, e.g., J. Y. Becker, L. L. Miller, and T. M. Siegel, *J. Am. Chem. Soc.*, **97**, 849, 853 (1975).
- P. Borrell and R. G. Norrish, *Proc. R. Soc. London, Ser. A*, **262**, 19 (1961); G. E. Hechler, A. E. Taylor, C. Jensen, D. Percirole, R. Jensen, and P. Fung, *J. Phys. Chem.*, **67**, 1 (1963); K. Clusius and D. Schanzer, *Chem. Ber.*, **75**, 1795 (1942).